Journal of Nuclear Medicine, published on May 26, 2022 as doi:10.2967/jnumed.122.264069

Repetitive early FAPI-PET acquisition comparing FAPI-02, FAPI-46 and FAPI-74: methodological and diagnostic implications for malignant, inflammatory and degenerative lesions

Frederik M. Glatting[1,2,3], Jorge Hoppner[1,4], Dawn P. Liew[1], Antonia van Genabith[1], Anna-Maria Spektor[1], Levin Steinbach[1], Alexander Hubert[1], Clemens Kratochwil[1], Frederik L. Giesel[1,5], Katharina Dendl[1], Hendrik Rathke[1,6], Hans-Ulrich Kauczor[4,7], Peter E. Huber[2,3], Uwe Haberkorn[1,7,8] and Manuel Röhrich[1,7]

Affiliations:

1 Department of Nuclear Medicine, University Hospital Heidelberg, Germany

2 Clinical Cooperation Unit Molecular and Radiation Oncology, German Cancer Research Center (DKFZ), Heidelberg, Germany

3 Department of Radiation Oncology, University Hospital Heidelberg, Germany.

4 Department of Diagnostic and Interventional Radiology, University of Heidelberg, Germany

5 Department of Nuclear Medicine, University Hospital Düsseldorf, Düsseldorf, Germany.

6 Department of Nuclear Medicine, The Inselspital, Bern University Hospital, University of Bern, Switzerland.

7 Translational Lung Research Center Heidelberg (TLRC), Member of the German Center for Lung Research DZL, Heidelberg, Germany

8 Clinical Cooperation Unit Nuclear Medicine, German Cancer Research Center (DKFZ), Heidelberg, Germany

Corresponding Author:

Manuel Röhrich

Im Neuenheimer Feld 400

69120 Heidelberg

Telephone: 0049 6221 56 7731

Fax: 0049 6221 56 5473

Email: manuel.roehrich@med.uni-heidelberg.de

ORCID-ID: 0000-0001-7609-243X

DECLARATIONS

Funding: This work was funded by the Federal Ministry of Education and Research, grant number 13N 13341.

Conflicts of interest: UH, CK and FLG have filed a patent application for quinoline based FAP targeting agents for imaging and therapy in nuclear medicine. UH, CK and FLG have shares of a consultancy group for iTheranostics. There are no other conflicts of interest.

Ethics approval: All procedures performed in studies involving human participants were in accordance with the ethical standards of the institutional and/or national research committee and with the 1964 Helsinki declaration and its later amendments or comparable ethical standards. This retrospective study was approved by the local institutional review board (study number S-115/2020).

ABSTRACT

Purpose:

FAPI-PET imaging targets FAP-positive, activated fibroblasts and is a promising imaging technique for various types of cancer and non-malignant pathologies. However, the discrimination between malignant and non-malignant FAPI-positive lesions based on static PET imaging with one acquisition timepoint can be challenging. Additionally, the optimal imaging timepoint for FAPI-PET has not been identified yet and even different FAPI tracer variants are currently used. In this retrospective analysis, we evaluate the diagnostic value of repetitive early FAPI-PET-imaging with FAPI-02, FAPI-46 and FAPI-74 for malignant, inflammatory and degenerative lesions and describe implications for future FAPI imaging protocols.

Methods:

Whole-body PET-Scans of 24 cancer patients were acquired at 10, 22, 34, 46 and 58 minutes after the administration of 150-250 MBq of ^{68}Ga-FAPI tracer molecules (8 Patients each regarding FAPI-02, FAPI-46 and FAPI-74). Detection rates and standardized uptake values (SUVmax and SUVmean) of healthy tissues, cancer manifestations and non-malignant lesions were measured and target-to-background ratios (TBR) versus blood and fat were calculated for all acquisition timepoints.

Results:

For most healthy tissues except fat and spinal canal, biodistribution analysis showed decreasing tracer uptake over time. 134 malignant, inflammatory/reactive and degenerative lesions were analysed. Detection rates were minimally reduced for the first two acquisition timepoints and remained on a constant high level from 34 to 58 minutes post injection (p.i.). The uptake of all three tracer variants was higher in malignant and inflammatory lesions than in degenerative lesions. FAPI-46 showed the highest uptake and TBRs in all pathologies. For all tracer variants, TBRs versus blood of all pathologies constantly increased over time and TBRs versus fat were constant or decreased slightly.

Conclusion:

FAPI-PET/CT is a promising imaging modality for malignancies and benign lesions. Repetitive early PET acquisition added diagnostic value for the discrimination of malignant and non-malignant FAPI-positive lesions. High detection rates and TBRs over time confirm that PET acquisition at timepoints earlier than 60 minutes p.i. deliver high contrast images. Additionally,

considering clinical feasibility, acquisition at 30 to 40 min p.i. could be a reasonable compromise. Different FAPI tracer variants show significant differences in their time-dependent biodistributional behaviour and should be selected carefully depending on the clinical setting.

Keywords: Fibroblast Activation Protein, FAPI, PET Cancer, Biodistribution

BACKGROUND

FAPI-PET imaging targets FAP-positive fibroblasts that occur in the tumour microenvironment as cancer-associated fibroblasts (*1-3*) as well as in benign pathologies such as fibrotic (*4,5*), reactive (*6*) and degenerative (*7*) processes. Numerous studies have demonstrated the great potential of FAPI-PET/CT for imaging of various malignancies (e.g. (*8,9*)) and non-malignant diseases, especially fibrotic and inflammatory (e.g. (*10-13*)) and degenerative diseases (*14,15*).

In the large majority of these studies, static PET images were acquired one hour post injection (p.i.) of the FAPI-tracer in analogy to F^{18}-FDG-PET. Some studies have evaluated FAPI-PET/CT imaging at different acquisition timepoints or dynamic FAPI-PET imaging (*13,16-19*), but the reported results are based on small numbers of patients and partially conflicting. To date, it is not clear which timepoint should be considered optimal for FAPI-PET acquisition. Moreover, a large variety of FAPI-tracer variants is currently in use at different centres and only a small number of preclinical (*20*) and clinical (e.g. (*6,8,16*)) studies have heretofore compared different FAPI-tracer variants regarding their biodistribution and imaging properties for different pathologies.

In this retrospective analysis, we evaluated a repetitive early FAPI-PET imaging protocol with PET acquisition at 10, 22, 34, 46 and 58 min after tracer application, wherein three FAPI-tracer variants (FAPI-02, FAPI-46 and FAPI-74) were applied in 8 patients respectively. The aim of this study was to describe the differential biodistribution and imaging properties of the three tracer variants over time for malignant, degenerative and inflammatory/reactive lesions and to determine an optimal timepoint for FAPI-PET acquisition with respect to imaging quality, optimal detection rate and optimized workflow.

PATIENTS AND METHODS

Patient Characterization

24 patients (aged 34 to 83 years, average 61 years) suffering from different types of cancer were examined by ^{68}Ga-FAPI-PET/CT. In order to avoid potential therapy effects on ^{68}Ga-FAPI-PET signalling, only patients without surgery, radiotherapy or chemotherapy within the last four weeks were examined. Median intervals between treatments and ^{68}Ga-FAPI-PET imaging were 13 months (range 1 to 240) for surgery, 29 months (range 2 to 260) for radiotherapy and 7 months (range 1 to 240) for chemotherapy. All patients were referred by their treating physicians for ^{68}Ga-FAPI-PET/CT due to clinical indications. All patients signed informed consent and thus agreed to the scientific evaluation of their personal data. This retrospective study was approved by the local institutional review board (study number S-115/2020). Patient characteristics and tracer variants for each patient are given in Supplemental Table 1.

Repetitive FAPI PET/CT imaging

Diagnostic imaging was performed under the conditions of the updated declaration of Helsinki, § 37 (unproven interventions in clinical practice) and in accordance with the German Pharmaceuticals Law §13 (2b) for medical reasons. FAPI tracers (FAPI-02, FAPI-46 and FAPI-74 with 8 patients each) were labelled with ^{68}Ga as previously described (*20*) and applied intravenously (80 nmol/GBq). PET/CT scans were performed within the first ten min after tracer injection with a Biograph mCT Flow™ PET/CT-Scanner (Siemens Medical Solutions) using the following parameters: slice thickness of 5 mm, increment of 3-4 mm, soft-tissue reconstruction kernel, care dose. PET scans were acquired exactly 10, 22, 34, 46 and 58 min post tracer administration (named as timepoint 1, 2, 3, 4 and 5) with a standardized field of view allowing whole-body scans within 12 min in 3D (matrix 200x200) in FlowMotion™ with 1.6 cm/min. Emission data were corrected for random, scatter and decay. Reconstruction was conducted with an ordered subset expectation maximization (OSEM) algorithm with 2 iterations/21 subsets and Gauss-filtered to a transaxial resolution of 5 mm at full-width half-maximum. Attenuation correction was performed using low-dose non-enhanced CT data.

Image analysis and quantification

Volumes of Interest (VOIs)

The quantitative assessment of standardized uptake values (SUV) using a volume of interest (VOI) technique was carried out by FMG and MR independently at first and followed by consensus. Tracer biodistribution in patients and uptake of pathologies were quantified by mean and maximum SUVs (SUVmean and SUVmax). Normal organs were evaluated using a sphere, placed inside the organ parenchyma, with a diameter of 5 mm for oral mucosa, parotid glands, thyroid, myocardium, pancreas, kidneys and spinal canal (C7), of 10 mm for blood, colon and fat tissue and of 15 mm for the brain, lungs, liver, spleen and muscles. Hereby, VOIs for blood were drawn at the beginning of the descending aorta on the first axial slide where the aortic arch was not visible anymore and VOIs for fat were drawn within gluteal fat tissue at the height of the acetabulum. Respecting SUV calculation of pathologies, spheric regions of interest were drawn around the lesions on FAPI-PET images acquired at 58 min p.i. and automatically adapted to a 3-dimensional volume by PMOD software at a 50-70% isocontour. All VOIs for normal tissues and pathologies were automatically transferred to the previous timepoints by PMOD software in order to achieve identical intra-individual VOIs.

We determined dominating tracer variants for each tissue by evaluating the mean absolute values of the SUVmax and SUVmean at the initial and following timepoints. Tracer variants with highest values and marked differences to the other two variants were considered dominant. If the differences between different FAPI tracers were not distinct, they were considered as approximately even.

Lesions were classified as malignant, inflammatory/reactive or degenerative based on clinical information and CT-morphology. Only lesions with highly suggestive characteristics for one of these classes were analysed. Detection rates for all classes of lesions were determined by MR, FMG and JH as previously described (*18*).

Increase, constant level or decrease of ^{68}Ga-FAPI-uptake were determined based on visual assessment and the trends of the mean absolute values of SUVmax or SUVmean over time.

Statistical Analysis

We performed descriptive analyses for patients and their characteristics. For determination of SUVs, median and range were used. The correlation of FAPI-uptake within or outside the lesions was determined by using a two-sided t-test. A p-value of <0.05 was defined as statistically significant. Excel version 2111 and Origin2021b were used for statistical analyses.

RESULTS

Patient cohort

Supplementary Table 1 summarizes demographic and clinical data of all patients.. Overall, one patient was treatment naïve, being initially metastasized. Out of the 23 patients with suspected recurrence or progression after resection and/or chemotherapy and/or radiotherapy, some patients showed evidence of a local tumour only (6), metastasis only (8) or both local tumour and metastasis (6) and no evidence of tumour (3).

Biodistribution

Figure 1 visualizes the biodistribution in terms of SUVmax and SUVmean over time for all physiological tissues. Organs are divided into highly (A) and lowly FAPI-avid (B). For most tissues, the SUVmax and SUVmean values decreased continuously, whereas SUVmax and SUVmean tended to increase for fat tissue and to remain constant for the spinal canal. By comparing the tissue uptake for the three different tracer variants, the dominating variant for each tissue is shown in Figure 2.

Figure 3 shows a representative clinical case for each tracer variant in terms of maximum intensity projection (MIP) images as well as fused axial ^{68}Ga-FAPI-PET/CT images showing blood pool, lungs and muscles. In accordance with the data of Figure 2, these typical examples underline the biodistribution of the tracer variants and show the highest uptake regarding blood for FAPI-02. However, the highest tracer uptake for muscle tissue can be observed for FAPI-46, according to the kinetics shown in Figure 1 and the data of Figure 2. Supplemental Figure 1 shows an inter-tissue comparison of the biodistribution at 34 and 58 min p.i..

Detection rate

Based on clinical information and CT-morphology, 134 lesions were classified as malignant, inflammatory or degenerative and used for further analysis. 3 lesions were labelled “other” as they could not be matched with one of the three classes and not further analysed. Table 1 summarizes all 137 lesions. For FAPI-02, 34 out of 49 (69.4%) lesions, for FAPI-46, 21 out of 52 (40.4%) and for FAPI-74 16 out of 36 (44.4%) were rated as malignant manifestations.

Table 1: Number of malignant (M), inflammatory/reactive (IR) or degenerative (D), pathologies for each radiotracer

Tracer variant	Pathology	Number [%]
FAPI-02	total	49 (100.0)
	M	34 (69.4)
	IR	4 (8.2)
	D	9 (18.4)
	other	2 (4.1)
FAPI-46	total	52 (100.0)
	M	21 (40.4)
	IR	8 (15.4)
	D	22 (42.3)
	other	1 (1.9)
FAPI-74	total	36 (100.0)
	M	16 (44.4)
	IR	9 (25.0)
	D	11 (30.6)
	other	0 (0.0)

Respecting FAPI-02 and FAPI-74, 2 malignant out of 47 total lesions (4.3%) and accordingly 1 malignant out of 36 total lesions (2.8%) could not be detected in the first timepoint imaging, but were detectable for the following four timepoints. For FAPI-46, a retroperitoneal liposarcoma remained undetected over all five timepoints. 2 degenerative out of 52 total lesions (3.8 %) were not detected at the first timepoint and 1 degenerative lesion (1.9%) was not seen at the second timepoint either. Both were detectable at the following timepoints. All inflammatory lesions were detected at all five timepoints for each tracer variant (Table 2).

Table 2: Detection rates and not detected lesions at different acquisition timepoints (M: malignant, IR: inflammatory/reactive, D: degenerative lesions)

Tracer variant	**Detection rate** [%] and not detected lesions				
	10 min	22 min	34 min	46 min	58 min
FAPI-02	**95,7** 2/34 M 0/4 IR 0/9 D	**100,0** 0/31* M 0/4 IR 0/6* D	**100,0** 0/34 M 0/4 IR 0/9 D	**100,0** 0/34 M 0/9 IR 0/9 D	**100,0** 0/34 M 0/4 IR 0/9 D
FAPI-46	**94,1** 1/21 M 0/8 IR 2/22 D	**96,1** 1/21 M 0/8 IR 1/22 D	**98,0** 1/21 M 0/8 IR 0/22 D	**98,0** 1/21 M 0/8 IR 0/22 D	**98,0** 1/21 M 0/8 IR 0/22 D
FAPI-74	**97,2** 1/16 M 0/9 IR 0/11 D	**100,0** 0/16 M 0/9 IR 0/11 D	**100,0** 0/16 M 0/9 IR 0/11 D	**100,0** 0/16 M 0/9 IR 0/11 D	**100,0** 0/16 M 0/9 IR 0/11 D

* In one patient with three malignant and three degenerative lesions image acquisition failed at timepoint 2.

Tracer uptake over time in malignant, inflammatory and degenerative lesions

The different types of lesions differed in their time-dependent uptake. Figure 4 provides an overview of the SUVmax and SUVmean kinetics of different types of lesions for the five acquisition times allowing a comparison between the tracer variants. Respecting FAPI-02, malignant lesions showed a slightly increasing uptake over time, whereas benign lesion tended to be constant or slightly decreasing. The absolute values between the three lesion types were similar.

For FAPI-46, malignant and inflammatory/reactive lesions show higher uptake than degenerative lesions. Moreover, the uptake within these lesions was higher than for FAPI-02 or FAPI-74. Additionally, regarding FAPI-46, malignant and inflammatory/reactive lesions featured a slope over time, whereas the uptake of degenerative lesions remained roughly unchanged.

FAPI-74 showed higher uptake in malignant and inflammatory lesions than in degenerative lesions. The uptake remained constant or only increased slowly for malignant and inflammatory lesions over time. However, the degenerative pathologies showed an increasing uptake over time finally approaching the level of the two other types of pathologies. This finding is demonstrated in Figure 5 by a ^{68}Ga-FAPI-74-PET/CT of a patient with a solitary hepatic metastasis, pancreatitis and an insertion-related tendinopathy in the right trochanter region. The uptake associated with the insertion-related tendinopathy increased over time, whereas the uptake of the hepatic metastasis and pancreatitis decreased slightly (Supplemental Table 2).

TBRs over time in malignant, inflammatory and degenerative lesions

As fat tissue showed an increasing FAPI-uptake for all three tracer variants over time, contrary to the other healthy tissues, and its uptake can be measured easily in a clinical setting, the SUVmax and SUVmean of fat tissue were used to calculate TBRs versus fat tissue in addition to TBRs versus blood. The corresponding graphs are depicted in Figure 6.

In comparison with FAPI-02 and FAPI-74, FAPI-46 showed a higher TBR versus blood as well as versus fat for malignant, inflammatory and degenerative lesions at all acquisition times. In contrast to the curve progression of the TBR versus blood, which increased over time for all tracer variants at different slopes regarding all three kinds of lesions, TBR versus fat tended to remain constant or to decrease slightly. This behaviour was particularly seen for FAPI-02 in inflammatory pathologies, while FAPI-74, still manifested an increase of the TBR versus fat values over time only for degenerative lesions.

DISCUSSION

In this retrospective analysis, we found differential time-dependent biodistributions for the three tracer variants FAPI-02, FAPI-46 and FAPI-74, implicating benefit of a thorough selection of the tracer variant depending on the tissue of interest and on the clinical setting. Furthermore, this study demonstrates the differential behaviour of malignant, inflammatory/reactive and degenerative lesions over time by considering the uptake and TBR versus blood and fat tissue.

Time-dependent biodistribution and FAPI tracer variants

Biodistribution analysis showed declining SUVmax and SUVmean values over time for all tissues except fat tissue (increase) and spinal cord (constant). The detection rate for each tracer variant was slightly reduced at 10 min p.i. for all variants and for FAPI-46 still at 22 min. p.i., but stable on a high level between 34 and 58 min p.i.. In order to optimize the selection of FAPI tracer variants, we identified the dominating tracer variant for each tissue. The tracer variant showing the lowest uptake, thus lowest background, within the healthy tissue is considered as a potential optimal variant. Of note, given the differential muscle/fat ratio of female and male patients and the variability of body mass, it could be of interest to perform an analysis of fat and muscle signalling with respect to sexes and body mass index in order to minimize background activity through optimal tracer variant selection. This may also be interesting with respect to reduction of radiation exposure, but would require a larger cohort than ours. However, as the magnitude of uptake at malignant and benign lesions and thereby the TBRs also affect the suitability of a tracer variant for a certain clinical context, uptake and TBR over time were analysed in malignant, inflammatory/reactive and degenerative lesions. Generally, the uptake was higher in malignant as well as inflammatory/reactive lesions than in degenerative lesions for all three tracer variants. However, different trends could be observed for the tracer variants. The slightly increasing or constant uptake of FAPI-02 over time could indicate a rapid uptake within the lesions and only slow washout process. Notably, FAPI-46 showed the highest uptake at pathologies of all tracer variants. Along with the observation that FAPI-46 showed a lower background activity in blood and other tissues, this tracer variant manifested the highest TBRs, too. While FAPI-46 featured a slightly increasing uptake within malignant and inflammatory/reactive lesions, there was an approximately constant uptake for degenerative lesions over time. FAPI-74 showed an

approximately constant level of uptake over time for malignant and inflammatory/reactive lesions, but an increase over time for degenerative lesions.

Uptake and TBRS in pathologies over time

Most previous studies analysing several acquisition timepoints demonstrated that the time-dependent differences are small within the period from 10 min p.i. to 180 min p.i. (*6,13,18,21*). Hu et al. observed a nonsignificant increase of SUVmax over time between 10 min and 60 min p.i., but calculated a significant increase of TBRs versus blood over time (*16*). In our study, we only found small differences in uptake between the five acquisition timepoints from 10 min p.i. to 60 min p.i.. Nevertheless, some trends could be concluded from the time-dependent uptake curves. Firstly, tracer uptake was higher in malignant and inflammatory lesions than in degenerative lesions for all three tracer variants. Additionally, the malignant, inflammatory/reactive and degenerative pathologies were distinguished from each other by their absolute values and by their uptake progression over time. TBRs versus blood of all pathologies constantly increased over time for all tracer variants, but at different slopes. In addition to the data presented here, we are planning to perform a separate analysis of this dataset focussed on different subclasses of malignant, inflammatory/reactive and degenerative lesions to identify further subgroups with differential uptake behaviours over time.

Diagnostic value of repetitive FAPI-Imaging and implications for FAPI-PET acquisition

^{68}Ga-FAPI-PET/CT is a promising imaging modality for the detection both of malignancies as well as for benign pathologies. Nevertheless, the optimal acquisition time has not been clearly determined yet. The current level of knowledge is ambiguous and inconsistent. On the one hand, one recently published study regarding ^{18}F-FAPI-42-PET/CT imaging of 22 patients concluded that the optimal acquisition time was 60 min p.i., arguing that TBR versus blood was small initially and increased over time and that some lesions were undetected early after tracer application due to the small initial TBR versus blood (*16*). At the same time, it was expressed that it might not be necessary to postpone the acquisition to later timepoints as the tumour detection was not improved at later timepoints. On the other hand, Ferdinandus et al. reasoned based on a retrospective study including 69 patients, who underwent ^{68}Ga-FAPI-46-PET imaging 10 and 60

min p.i., that detection rates at both acquisition timepoints did not differ(*18*). Due to the improved feasibility and scan volume, the authors decided to implement early acquisition timepoints in future PET-protocols.

Contrary to this conclusion and partly agreeing with the results of Hu et al., our study showed that the detection rate was slightly reduced at 10 min p.i. (mainly caused by undetected malignant and degenerative lesions), thus arguing against performing clinical interpretation based on early timepoint acquisition at 10 min p.i. only. Along with the increasing TBR versus blood and constant TBR versus fat over time, our finding suggested the later timepoints would be favourable concerning optimal clinical interpretations of PET/CT imaging. Taking clinical practicability and feasibility into account along with a sufficient detection rate, acquisition at 30 to 40 min p.i. is what we recommend and appears to be a reasonable compromise.

Limitations

Several limitations of our analysis must be considered. One limitation arises from the relatively low number of 24 patients included. Thus, conclusions on our data should be drawn with caution. A second limitation is the absence of histological confirmations of the lesions. Our classification of pathologies had to performed on the basis of CT-morphological anomalies. Thirdly, VOIs for the biodistribution analysis as well as for pathologies were defined using the dataset of the last acquisition timepoint and subsequently transferred to the previous timepoints in order to achieve identical intra-individual VOIs. This can lead to an uncertainty caused by movement artefacts within the first four acquisition timepoints, even though datapoints with visually obvious spatial differences were excluded from the dataset. Further due to the small number of degenerative lesions using FAPI-74, the surprising finding of the markedly increasing uptake over time for degenerative lesions has to be interpreted carefully. Another limitation is related to the heterogeneity of the patient cohorts per tracer variant. Although emphasis was put on pancreatic carcinoma within the patient groups, rarer entities of malignancies such as liposarcomas, that are known to show FAP expression not only by cancer associated fibroblasts, but also by neoplastic cells (*22*) were included, which may have reduced the inter-group comparability. Since the results between tumour entities did not differ markedly, our conclusions could be relevant beyond the considered tumour entities.

CONCLUSION

FAPI-PET/CT is a promising innovative imaging modality for various malignancies as well as for various benign conditions. Repetitive early PET acquisition added diagnostic value for the discrimination of malignant and non-malignant FAPI-positive lesions. TBRs and high detection rates over time confirm that PET acquisition at timepoints earlier than 60 min p.i. deliver high contrast images. According to our findings by taking clinical practicability and feasibility into consideration along with a sufficient detection rate, we would recommend acquisition at 30 to 40 min p.i.. Different FAPI tracer variants show significant differences in their time-dependent biodistributional behaviour and should be selected carefully depending on the clinical setting.

Acknowledgements

We thank Ms. Oda Landmann-Fothergill for her language corrections.

KEY POINTS

Question: To deliver a rationale for the selection of optimal tracer variants and acquisition time of FAPI-PET imaging.

Pertinent Findings: Background activity of most tissues decreased over time. Detection rates of pathologies were minimally reduced for early acquisition timepoints. FAPI-46 showed the highest uptake in all pathologies. For all tracer variants and pathologies, TBRs versus blood increased over time and TBRs versus fat were constant or decreased slightly.

Implications for Patient Care: FAPI tracer variants show significant differences in their time-dependent biodistributional behaviour and should be selected carefully depending on the clinical setting.

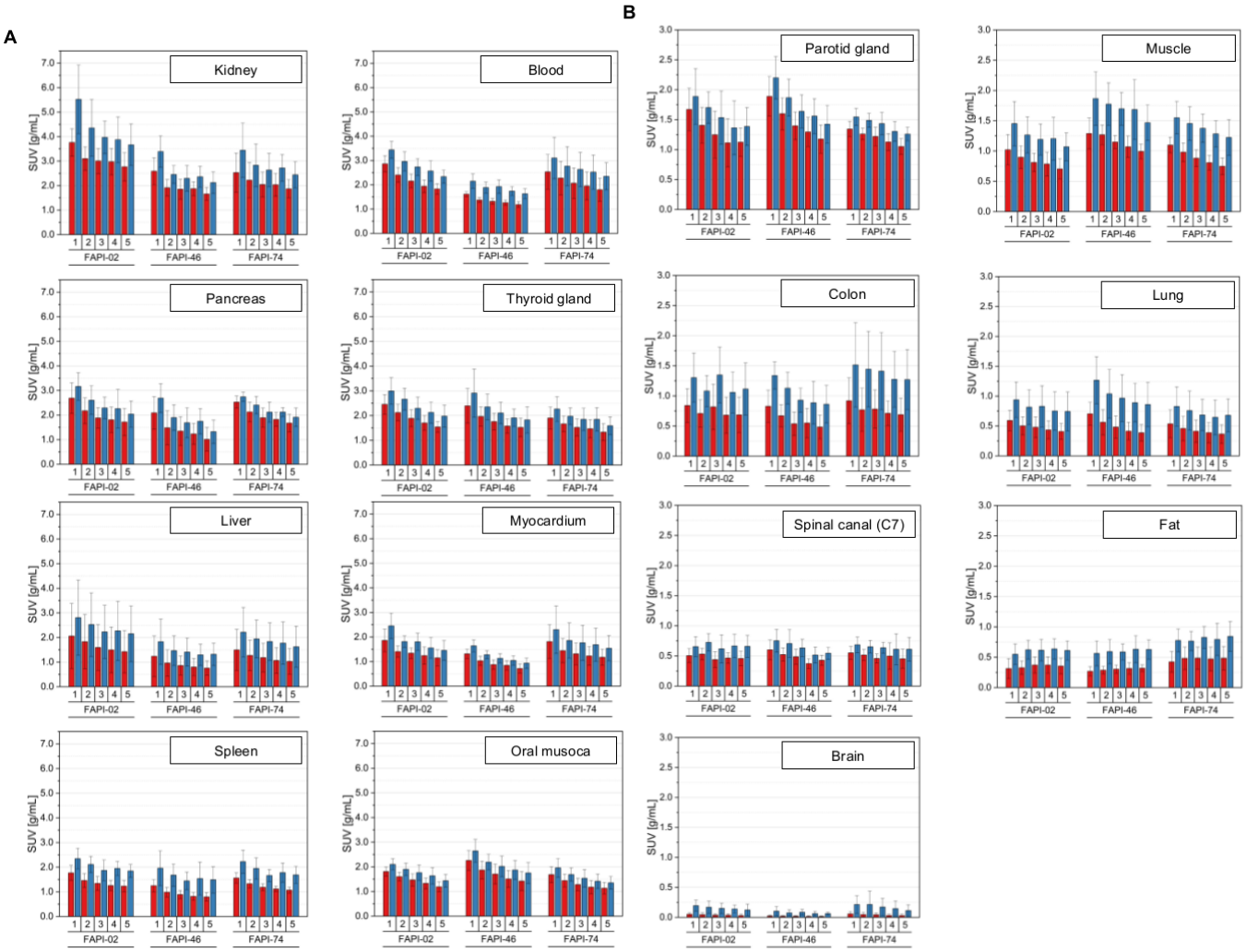

Figure 1: (A-B) Biodistribution analysis (SUVmean (red bar) and SUVmax (blue bar) values +/- standard deviation) of 24 patients, eight patients per FAPI tracer variant, with high (A) and low (B) uptake tissues over time with acquisition timepoints 10 min (1), 22 min (2), 34 min (3), 46 min (4) and 58 min (5) after application of ^{68}Ga-FAPI tracer variants of either FAPI-02, FAPI-46 or FAPI-74.

Figure 2

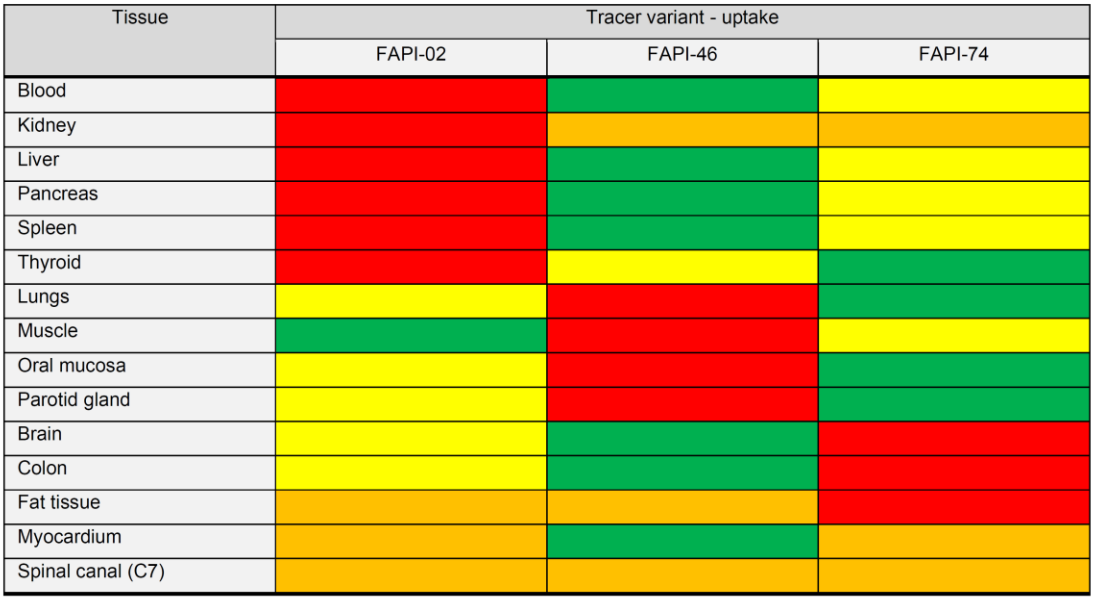

Tissue	Tracer variant - uptake		
	FAPI-02	FAPI-46	FAPI-74
Blood			
Kidney			
Liver			
Pancreas			
Spleen			
Thyroid			
Lungs			
Muscle			
Oral mucosa			
Parotid gland			
Brain			
Colon			
Fat tissue			
Myocardium			
Spinal canal (C7)			

Figure 2: Dominating FAPI tracer variant for each considered tissue (red colour indicating highest, yellow medium and green lowest uptake, orange indicating approximately even uptake).

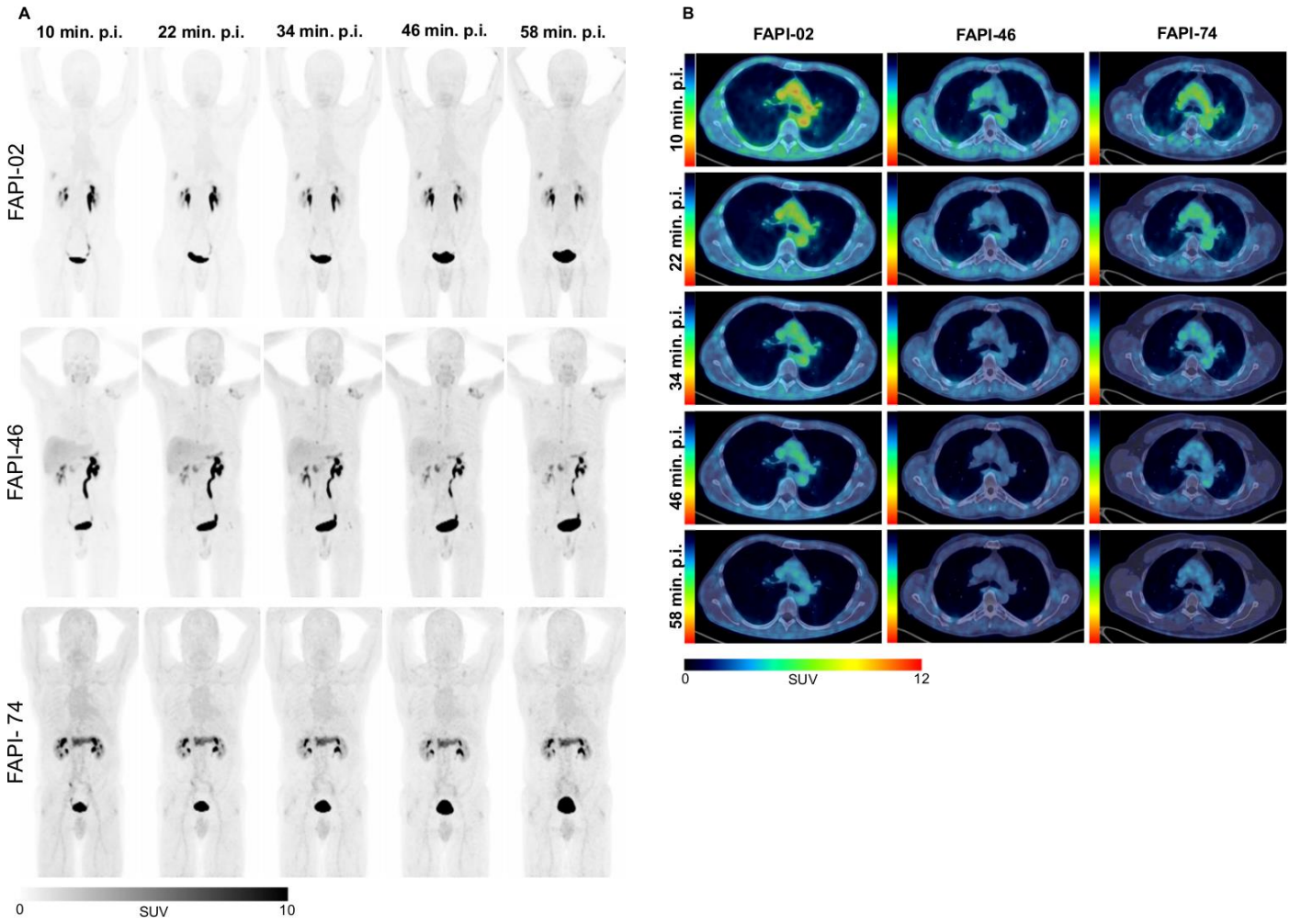

Figure 3: A Representative maximum injection projection (MIP) images of ^{68}Ga-FAPI-PET/CT imaging for FAPI-02 (upper row, 56 year old male patient with resected pancreatic carcinoma, staging for metastases, no local recurrence, single hepatic metastasis), FAPI-46 (middle row, 64 year old male patient with pancreatic cancer, staging with suspected local recurrence, no metastases) or FAPI-74 (lower row, 60 year old male patient with pancreatic carcinoma, staging in advance of radiation therapy, primary, single hepatic metastasis) over time with acquisition timepoints 10 min (1), 22 min (2), 34 min (3), 46 min (4) and 58 min (5) after application. **B** Representative axial fused ^{68}Ga-FAPI-PET/CT images of the upper thorax showing tracer uptake for blood, muscle and lungs over time with acquisition timepoints 10 min (1), 22 min (2), 34 min (3), 46 min (4) and 58 min (5) after application for FAPI-02 (left column, 56 year old male patient with resected pancreatic carcinoma, staging for metastases, no local recurrence, single hepatic

metastasis), FAPI-46 (middle column, 58 year old male patient with a retroperitoneal liposarcoma, staging in advance of neoadjuvant radiation therapy, primary, three metastases) or FAPI-74 (60 year old male patient with pancreatic carcinoma, staging in advance of radiation therapy, primary, single hepatic metastasis).

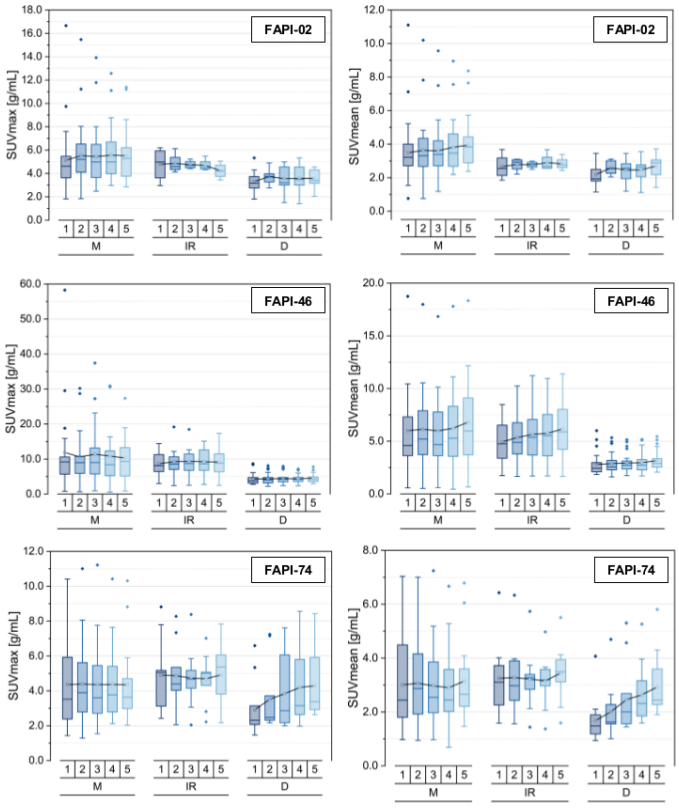

Figure 4: SUVmax and SUVmean values of malignant(M), inflammatory/reactive(IR) or degenerative(D) pathologies over time at 10 min (1), 22 min (2), 34 min (3), 46 min (4) and 58 min (5) after injection of ^{68}Ga-FAPI tracer of either FAPI-02, FAPI-46 or FAPI-74. Boxes represent the interquartile range (IQR), whiskers the range of 1.5 IQR, horizontal line within the box indicates the median and small box the mean. Data outliers are shown separately within graph. Trending lines regarding mean are shown.

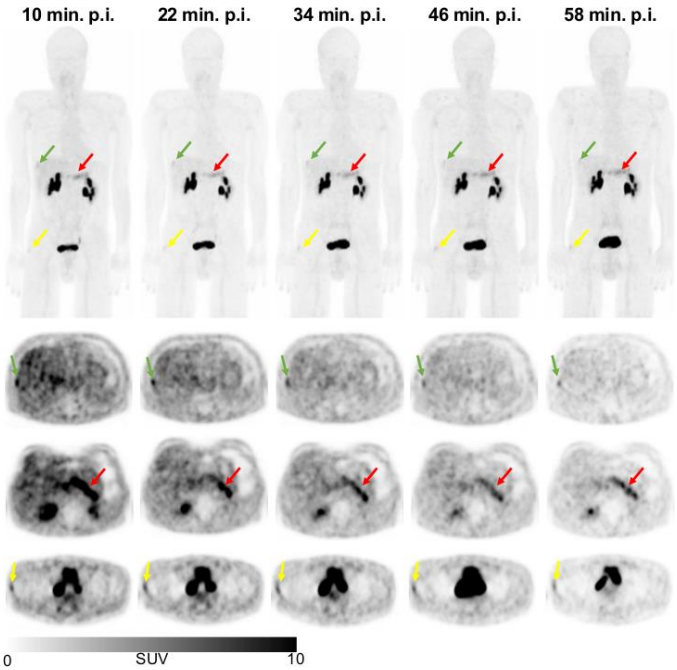

Figure 5:

Exemplary maximum injection projection (MIP, first row) and axial fused PET/CT images of ^{68}Ga-FAPI-74-PET/CT scans for a 56 year-old male patient with pancreatic carcinoma after resection (no local recurrence, 4 metastases) over time with acquisition timepoints 10 min (1), 22 min (2), 34 min (3), 46 min (4) and 58 min (5) after application. Clinically, the patient showed a hepatic metastasis (green arrow, second row, malignant manifestation), a pancreatitis-related uptake (red arrow, third row, inflammatory lesion) and an insertion-related tendinopathy in the right trochanter region (yellow arrow, fourth row, degenerative lesion).

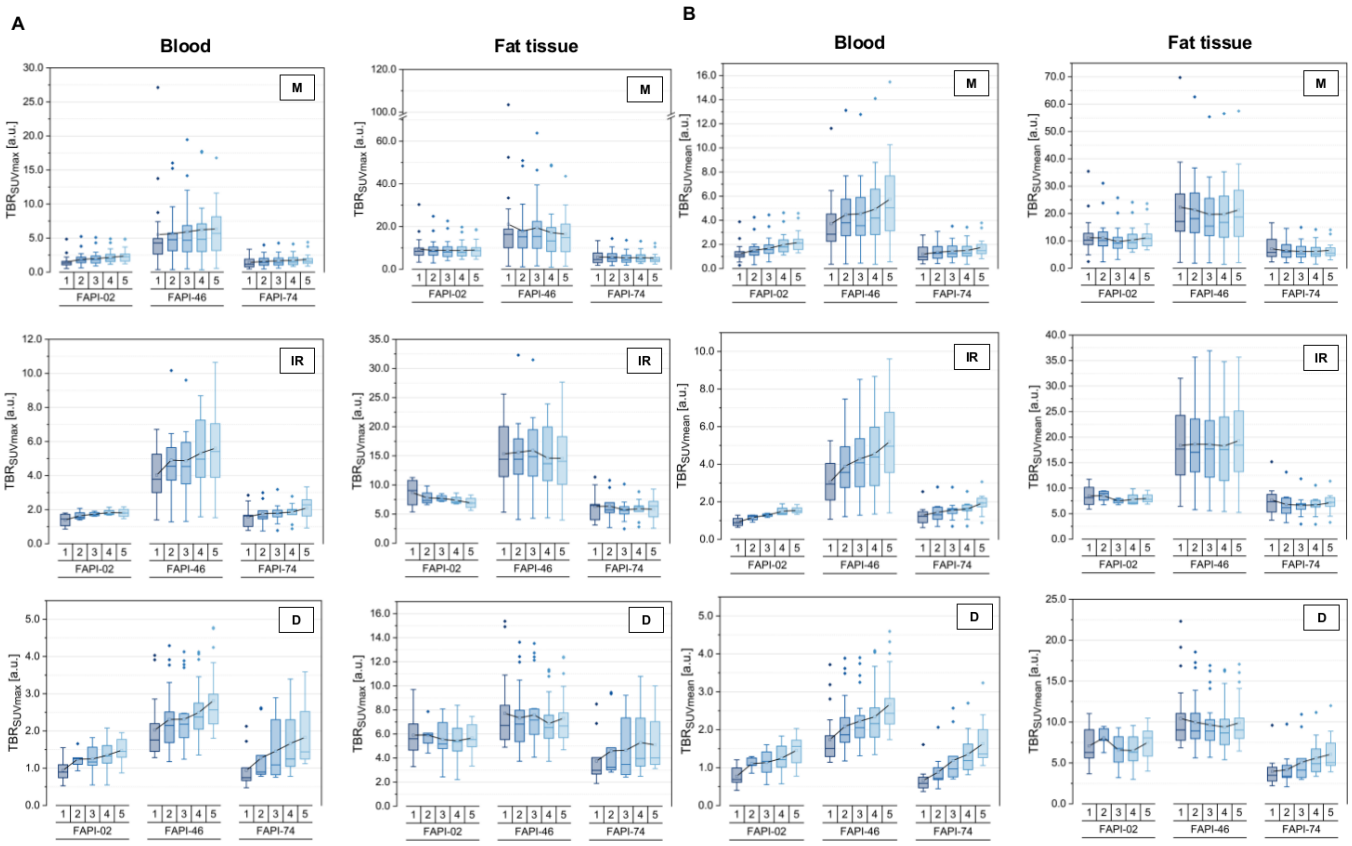

Figure 6: **(A-B)** Target to Background ratios (TBRs) for SUVmax (A) and SUVmean (B) values regarding malignant (M), inflammatory/reactive (IR) or degenerative (D) pathologies versus blood and versus fat tissue for the three ^{68}Ga-FAPI tracer variants FAPI-02, FAPI-46 an FAPI-74 over time with acquisition timepoints 10 min (1), 22 min (2), 34 min (3), 46 min (4) and 58 min (5) after injection. Boxes represent the interquartile range (IQR), whiskers the range of 1.5 IQR, horizontal line within the box indicates the median and small box the mean. Data outliers are shown separately within graph. Trending lines regarding mean are shown.

REFERENCES

1. LeBleu VS, Kalluri R. A peek into cancer-associated fibroblasts: origins, functions and translational impact. *Dis Model Mech.* 2018;11.

2. Kalluri R. The biology and function of fibroblasts in cancer. *Nat Rev Cancer.* 2016;16:582-598.

3. Sahai E, Astsaturov I, Cukierman E, et al. A framework for advancing our understanding of cancer-associated fibroblasts. *Nat Rev Cancer.* 2020;20:174-186.

4. Henderson NC, Rieder F, Wynn TA. Fibrosis: from mechanisms to medicines. *Nature.* 2020;587:555-566.

5. Affo S, Yu LX, Schwabe RF. The Role of Cancer-Associated Fibroblasts and Fibrosis in Liver Cancer. *Annu Rev Pathol.* 2017;12:153-186.

6. Rohrich M, Naumann P, Giesel FL, et al. Impact of (68)Ga-FAPI-PET/CT imaging on the therapeutic management of primary and recurrent pancreatic ductal adenocarcinomas. *J Nucl Med.* 2020.

7. Pap T, Dankbar B, Wehmeyer C, Korb-Pap A, Sherwood J. Synovial fibroblasts and articular tissue remodelling: Role and mechanisms. *Semin Cell Dev Biol.* 2020;101:140-145.

8. Kratochwil C, Flechsig P, Lindner T, et al. (68)Ga-FAPI PET/CT: Tracer Uptake in 28 Different Kinds of Cancer. *J Nucl Med.* 2019;60:801-805.

9. Chen H, Pang Y, Wu J, et al. Comparison of [(68)Ga]Ga-DOTA-FAPI-04 and [(18)F] FDG PET/CT for the diagnosis of primary and metastatic lesions in patients with various types of cancer. *Eur J Nucl Med Mol Imaging.* 2020;47:1820-1832.

10. Luo Y, Pan Q, Yang H, Peng L, Zhang W, Li F. Fibroblast activation protein targeted PET/CT with (68)Ga-FAPI for imaging IgG4-related disease: comparison to (18)F-FDG PET/CT. *J Nucl Med.* 2020.

11. Schmidkonz C, Rauber S, Atzinger A, et al. Disentangling inflammatory from fibrotic disease activity by fibroblast activation protein imaging. *Ann Rheum Dis.* 2020;79:1485-1491.

12. Zhou Y, Yang X, Liu H, et al. Value of [(68)Ga]Ga-FAPI-04 imaging in the diagnosis of renal fibrosis. *Eur J Nucl Med Mol Imaging.* 2021;48:3493-3501.

13. Rohrich M, Leitz D, Glatting FM, et al. Fibroblast Activation Protein-Specific PET/CT Imaging in Fibrotic Interstitial Lung Diseases and Lung Cancer: A Translational Exploratory Study. *J Nucl Med.* 2022;63:127-133.

14. Qin C, Song Y, Liu X, et al. Increased uptake of (68)Ga-DOTA-FAPI-04 in bones and joints: metastases and beyond. *Eur J Nucl Med Mol Imaging.* 2021.

15. Liu H, Wang Y, Zhang W, Cai L, Chen Y. Elevated [(68)Ga]Ga-DOTA-FAPI-04 activity in degenerative osteophyte in a patient with lung cancer. *Eur J Nucl Med Mol Imaging.* 2020.

16. Hu K, Wang L, Wu H, et al. [(18)F]FAPI-42 PET imaging in cancer patients: optimal acquisition time, biodistribution, and comparison with [(68)Ga]Ga-FAPI-04. *Eur J Nucl Med Mol Imaging.* 2021.

17. Wang S, Zhou X, Xu X, et al. Dynamic PET/CT Imaging of (68)Ga-FAPI-04 in Chinese Subjects. *Front Oncol.* 2021;11:651005.

18. Ferdinandus J, Kessler L, Hirmas N, et al. Equivalent tumor detection for early and late FAPI-46 PET acquisition. *Eur J Nucl Med Mol Imaging.* 2021;48:3221-3227.

19. Geist BK, Xing H, Wang J, et al. A methodological investigation of healthy tissue, hepatocellular carcinoma, and other lesions with dynamic (68)Ga-FAPI-04 PET/CT imaging. *EJNMMI Phys.* 2021;8:8.

20. Loktev A, Lindner T, Burger EM, et al. Development of Fibroblast Activation Protein-Targeted Radiotracers with Improved Tumor Retention. *J Nucl Med.* 2019;60:1421-1429.

21. Rohrich M, Syed M, Liew DP, et al. (68)Ga-FAPI-PET/CT improves diagnostic staging and radiotherapy planning of adenoid cystic carcinomas - Imaging analysis and histological validation. *Radiother Oncol.* 2021;160:192-201.

22. Dohi O, Ohtani H, Hatori M, et al. Histogenesis-specific expression of fibroblast activation protein and dipeptidylpeptidase-IV in human bone and soft tissue tumours. *Histopathology.* 2009;55:432-440.

GRAPHICAL ABSTRACT

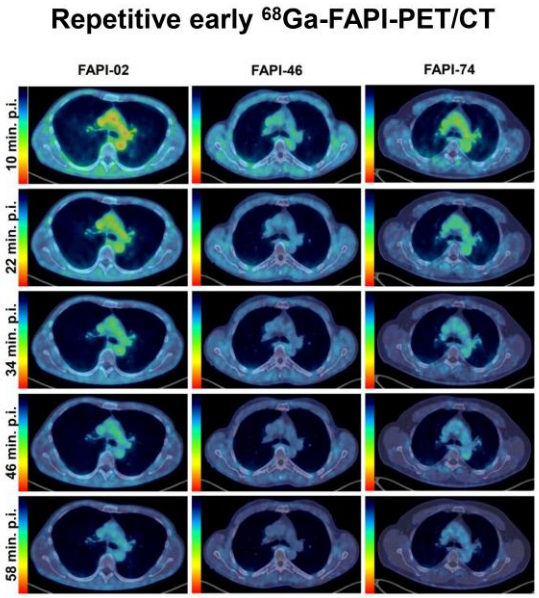

SUPPLEMENTAL MATERIAL

Supplemental Table 1: Patient characteristics and FAPI-PET/CT imaging features

Patient number	Age	Sex	Diagnosis	Previous treatments	Clinical setting	Tracer variant	Malignant findings in ^{68}Ga-FAPI-PET/CT
1	77	M	Transitional cell carcinoma of the urinary bladder	Resection of urinary bladder	Restaging	FAPI-02	No manifestations
2	74	F	Mamma carcinoma & renal cell carcinoma (RCC)	*Mamma carcinoma:* ablatio mammae, radiation therapy, tamoxifen and goserelin, trastuzumab and exemestane, resection of metastasis (right axilla) *RCC:* resection, analgesic radiation therapy of sternum, Letrozole and Palbociclib	Progress monitoring	FAPI-02	No local recurrence, 10 metastases
3	67	M	Pancreatobiliary adenocarcinoma of the papilla (pancreatic head)	Whipple operation	Suspected recurrence	FAPI-02	Local recurrence, 6 metastases
4	60	M	Appendix carcinoma	Hemicolectomy, HIPEC (Oxaliplatin), 5-FU, leucovorin, segment resection of small intestine, FOLFOX, changed to FOLFIRI, Bevacizumab	Progress monitoring	FAPI-02	No clear local recurrence, 8 metastases
5	71	F	Mamma carcinoma	Ablatio mammae, adjuvant radiation therapy, doxorubicin, partial hepatectomy with local perfusion of mitomycin C and epirubicin, tamoxifen, letrozole, resection of local recurrence, doxorubicin and paclitaxel	Suspected recurrence	FAPI-02	No clear local recurrence, 3 metastases
6	56	M	Ductal adenocarcinoma of the pancreatic head	FOLFIRINOX, pylorus-preserving Whipple operation, cholecystectomy, p53- & neo-epitope vaccination	Progress monitoring	FAPI-02	No local recurrence, single metastasis
7	62	M	Ductal adenocarcinoma of the pancreatic corpus	Left pancreatectomy, splenectomy, FOLFIRINOX, atypical resection of right upper lobe	Recurrence suspected	FAPI-02	Local recurrence, no metastasis

8	55	M	Ductal adenocarcinoma of the pancreatic head and corpus	Total pancreatectomy, splenectomy, adjuvant mFOLFIRINOX/FOLFIRINOX	Progress monitoring	FAPI-02	Local recurrence, 3 metastases
9	34	F	Colorectal carcinoma	Recto-sigmoidectomy, resection of posterior vaginal wall, ureterolysis, FOLFOXIRI	Progress monitoring	FAPI-46	No local recurrence, 1 metastasis
10	58	M	Liposarcoma (retroperitoneal)	None, CT-guided biopsy	Primary staging	FAPI-46	Primary, 3 metastases
11	83	F	Oesophageal carcinoma	Endoscopy with biopsy, neoadjuvant radio-chemotherapy (CROSS-Studie; systemic therapy: Carboplatin/Paclitaxel), thoracoabdominal resection of oesophagus with oesophago-gastrostomy, SBRT of right lower lobe	Progress monitoring/ suspected recurrence	FAPI-46	No local recurrence, no metastases
12	63	M	Pancreatobiliary adenocarcinoma of the pancreatic head	ERCP with stent implantation, FOLFIRINOX, surgical exploration	Progress monitoring	FAPI-46	Primary, no metastases
13	58	M	Nasopharyngeal carcinoma	Biopsy, neoadjuvant chemotherapy with Cisplatin & Docetaxel, panendoscopy with biopsies, resection of nasopharyngeal carcinoma	Suspected recurrence	FAPI-46	Local recurrence, both oro- and nasopharynx, no metastases
14	45	M	Transitional cell carcinoma of the urinary bladder	Transurethral resection of urinary bladder, neoadjuvant chemotherapy (gemcitabine, cisplatin), laparoscopic nephroureterectomy, median laparotomy, radical cystoprostatectomy, lympadenectomy and ileumneobladder, gemcitabine/nab-Paclitaxel, ileocaecal resection	Suspected recurrence	FAPI-46	No local recurrence, 5 metastases
15	64	M	Ductal adenocarcinoma of the pancreatic head	FOLFIRINOX, partial pylorus-preserving pancreato-duodenectomy with end-to-side duodeno-jejunostomy, cholecystectomy, mFOLFIRINOX	Suspected local recurrence	FAPI-46	Local recurrence, no metastases
16	66	M	Ductal adenocarcinoma of the pancreatic head	Pancreato-duodenectomy analogous to Whipple, FOLFIRINOX, gemcitabine/paclitaxel	Progress monitoring	FAPI-46	Local recurrence, 5 metastases
17	79	M	Ductal adenocarcinoma of the pancreatic head	Adhesiolysis, pylorus-perserving duodeno-hemipancreatectomy	Suspected recurrence	FAPI-74	Local recurrence, 2 metastases

18	49	M	ACC	Bronchoscopy with biopsies, radiation therapy (bimodal: C12 carbon ions as booster), resection of solitary lung metastasis in subsegement 9 left lung	Progress monitoring	FAPI-74	Primary, no metastases
19	66	M	Ductal adenocarcinoma of the pancreatic head	Whipple operation, FOLFIRINOX, ERCP with stent implantation	Suspected recurrence	FAPI-74	Local recurrence, single metastasis
20	69	F	Uterine sarcoma	Explorative laparotomy, hysterectomy with adnexectomy on both sides, omentectomy, extirpation of pelvic and paraaortic lymph nodes, ureterolysis, ureterresection, sigmaresection, ileostoma, re-resection of vaginal stump, IORT	Suspected recurrence	FAPI-74	Primary, no metastases
21	42	F	SPN of the pancreas	Total pylorus-preserving pancreatectomy, splenectomy, cholecystectomy, hemihepatectomy	Progress monitoring	FAPI-74	No local recurrence, 2 metastases
22	51	F	Liposarcoma	Hemicolectomy, nephrectomy, cholecystectomy, partial hepatectomy, multiple recurrence surgery, tumour extirpation at liver hilum, omentectomy, partial resection of diaphragm, extirpation of liposarcoma recurrence, resection of terminal ileum with ileotransversostomy, IORT at bifurcation of aorta abdominalis, resection of abdominal wall, tumour-specific vaccination, explorative laparotomy with adhesiolyis, partial ileum resection, Ileoileostomy	Suspected recurrence	FAPI-74	No manifestation
23	60	M	Ductal adenocarcinoma of the pancreatic head and corpus	Endosonography with fine needle punction, FOLFIRINOX	Primary staging	FAPI-74	Primary, single metastasis
24	56	M	Ductal adenocarcinoma of the pancreatic head	neoadjuvant chemotherapy FOLFIRINOX, Whipple operation, radiation therapy, gemcitabine/paclitaxel	Suspected recurrence	FAPI-74	No local recurrence, four metastases

Abbreviations: RCC - renal cell carcinoma; ACC - adenoid cystic carcinoma; SPN - Solid pseudopapillary neoplasia of the pancreas; HIPEC - intraperitoneal hyperthermic chemoperfusion; 5-FU – fluorouracil; FOLFOX - chemotherapy regimen, including **fol**inic acid, 5-**F**U and **ox**aliplatin; FOLFIRI - chemotherapy regimen, including **fol**inic acid, 5-**F**U and **iri**notecan; (m)FOLFIRINOX – chemotherapy regimens, including **fol**inic acid, 5-**F**U, **irin**otecan and **ox**aliplatin; FOLFOXIRI - chemotherapy regimen, including **fol**inic acid, 5-**F**U, **ox**aliplatin and **iri**notecan; SBRT - stereotactic body radiation therapy; ERCP - endoscopic retrograde cholangiopancreatography, IORT - intraoperative radiation therapy

Supplemental Figure 1

A

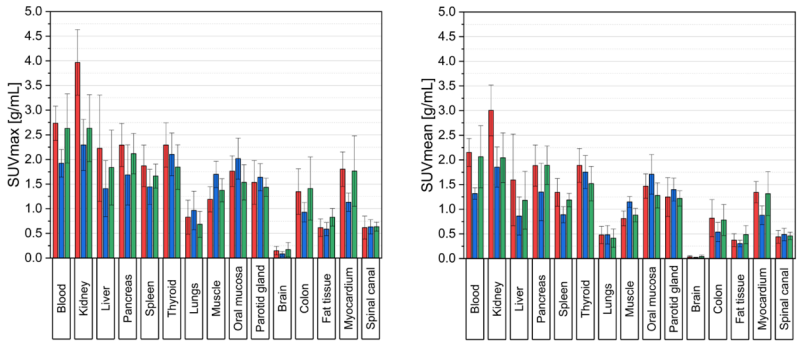

B

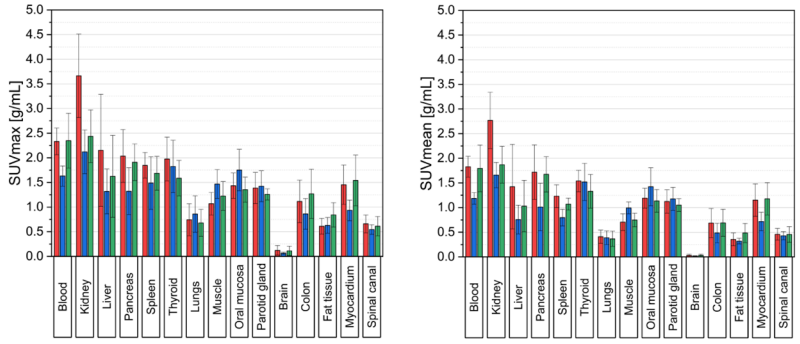

Supplemental Figure 1: Biodistribution analysis (SUVmax and SUVmean) in healthy tissues of 8 patients per tracer variant of FAPI-02 (red bar), FAPI-46 (blue bar) or FAPI-74 (green bar) based on ^{68}Ga-FAPI-PET imaging at the acquisition timepoints of 34 min (**A**) and 58 min (**B**) post injection. Results are shown as mean +/- standard deviation.

Supplemental Table 2: ^{68}Ga-FAPI-74-uptake (SUVmean and SUVmax) of the pathologies (pancreatitis, hepatic metastasis, insertion-related tendinopathy) visualized in Figure 5 over time with acquisition timepoints 10 min (1), 22 min (2), 34 min (3), 46 min (4) and 58 min (5) after application

Timepoint	Pancreatitis		Hepatic metastasis		Insertion-related tendinopathy	
	SUVmean	SUVmax	SUVmean	SUVmax	SUVmean	SUVmax
1	4,0091	7,791	2,7129	3,6625	1,3724	2,2142
2	3,9752	7,3352	2,7747	3,6328	1,5967	2,4709
3	3,737	5,8478	2,5646	3,4806	1,7971	2,6101
4	3,5273	5,9745	2,2256	2,8599	1,8498	3,1478
5	3,8195	6,0607	2,3146	3,1523	1,8979	2,8765